Heat capacity, adsorption isotherms, and quasielastic neutron scattering measurements of bilayer deuterium hydride adsorbed on graphite

Yuan-Ming Liu,* Peter S. Ebey,† Oscar E. Vilches, and J. G. Dash
Department of Physics, University of Washington, Seattle, Washington 98195-1560

Michel Bienfait and Jean-Marc Gay
CRMC2-CNRS, Campus de Luminy, Case 913, 13288 Marseille, Cedex 9, France

Gerrit Coddens
Laboratoire Leon Brillouin, CEN de Saclay, 91191 Gif-sur-Yvette Cedex, France
(Received 22 January 1996)

Bilayer films of deuterium hydride (HD) adsorbed on exfoliated graphites have been studied using heat capacity, adsorption isotherms, and quasielastic neutron scattering (QENS) measurements. The second layer of HD shows solid (S), liquid (L), and gaseous (G) [vapor (V)] phases, with two-dimensional (2D) characteristics. We determined the S-L-V triple line at $T_t(2D)=8.44$ K, and the L-V critical temperature at $T_c(2D)=11.45$ K. QENS identified the L phase and measured its translation diffusion coefficient $D_T(\approx 10^{-5}$ $cm^2\ s^{-1}$ at 9.25 K). Isosteric heats, latent heat, and entropy change at melting, and solid Debye temperatures are calculated. The results are used to construct a general graph of critical and triple points of adsorbed gases as a function of their quantum parameter. [S0163-1829(96)00233-0]

I. INTRODUCTION

The three nonradioactive hydrogen isotopic molecules, hydrogen (H_2), deuterium hydride (HD), and deuterium (D_2) are the substances with the lowest solid-liquid-vapor (S-L-V) triple points in three dimensions (3D). The small molecule-molecule attraction [the Lennard-Jones depth (ε) of the hydrogen-hydrogen potential is 37 K] and the small molecular masses (large zero-point kinetic energy) are responsible for their very low triple-point temperatures, respectively, $T_t(3D)$, of 13.8, 16.8, and 18.7 K.

The isotopic molecule HD has special properties which make it unique. It is a fermion [$T_F(2D)=1.3$ K for a gas of surface density 0.025 $Å^{-2}$], while H_2 and D_2 are bosons. Because it is an asymmetric rotor it has no orthopara varieties (and the associated conversion of one to the other as the temperature changes). It also has a large incoherent neutron-scattering cross section which makes it ideal for the study of diffusion by quasielastic neutron scattering (QENS).

Single monolayers of H_2, HD, and D_2 adsorbed on graphite have been studied extensively by a variety of techniques. A review of the known phases and phase transitions for each molecular isotope has been written by Wiechert.[1] Bilayer films of H_2 and D_2 on graphite have also been studied by Wiechert,[2] while bilayer films formed by plating one layer of D_2 or HD on the same substrate, then depositing H_2 on the plated system have been studied by Liu *et al.*[3,4] The interest in the bilayer systems comes from the observation that the second layer on top of a solid first layer shows phase transitions which delineate density-temperature phase diagrams similar to their respective 3D counterparts but with much lower critical and triple-point temperatures, as expected from quantum effects and dimensionality for purely two-dimensional (2D) systems. For example, S-L-V 2D triple points measured in Ref. 2 using heat capacity are at 5.96 K for H_2 and 11.04 K for D_2. From Ref. 3, also using heat capacity, the mixed system of H_2/D_2/gr has the second-layer triple point at 5.74 K, while the other mixed system, H_2/HD/gr has it at an average temperature of 6.3 K. If the nature of the liquid phase was confirmed, these would be, so far, the lowest S-L-V coexistence points found in 2D.

The only other systems where somewhat similar phases are observed are bilayers of H_2 and HD adsorbed on MgO, with critical and triple temperatures higher than on graphite (see Sec. IV and Fig. 12). For H_2/H_2/MgO, heat-capacity measurements found $T_t(2D)=7.2$ K.[5] For HD/HD/MgO adsorption isotherms estimate $T_t(2D)\approx 9.9$ K.[6]

QENS measurements on HD thick films adsorbed on graphite[7] and on two to five layers adsorbed on MgO (Ref. 8) have determined mobilities of the order of magnitude expected for liquids, as well as mobile fractions in reasonable agreement with the thermodynamic phase diagrams. In particular, a liquid second layer is seen above the estimated $T_t(2D)$.[8] Complementary evidence for a mobile second layer of HD on MgO has been obtained using nuclear magnetic resonance.[9]

Additional interest in HD comes from evidence that as a first layer plating for the adsorption of H_2, or as an overlayer on D_2, it shows interlayer mixing as the temperature increases.[4] Recent studies of both ^{4}He and ^{3}He adsorbed on hydrogen-plated graphite have actually used two layers of HD as the plating substrate,[10] a choice appropriate to eliminating orthopara conversion (and heating) for very low temperature studies of the helium isotopes. Further understanding of the role of the substrate can be achieved by carefully mapping the possible phases of HD/HD/gr.

In this paper we present results from combined heat-capacity, adsorption isotherms, and QENS measurements on

bilayer HD physisorbed on graphite. With the thermodynamic measurements we determined the outline of the second-layer phase diagram and found $T_t(2D) \approx 8.44$ K and $T_c(2D) \approx 11.45$ K. The QENS measurements identified that the second-layer HD is indeed a liquid above 8.44 K and determined its mobility . The adsorption isotherms were extended onto the third and fourth layers to find layering critical points and heats of adsorption. An analysis of the data and a placement of the findings in the context of corresponding states ends the paper.

II. EXPERIMENT

The experiments were conducted on three different setups, with exfoliated graphite cells adapted to each technique, and in the case of the QENS, with different cells on different experiments. The various exfoliated graphites were obtained from either Union Carbide Co., Carbon Products Division (graphite foam and exfoliated uncompressed crystallites) or Carbon Lorraine (Papyex). Papyex is commercially available, while the uncompressed exfoliated crystallites and foam (sheets about 5 mm thick) were kindly given to us a long time ago by the Union Carbide Corp.

The adiabatic heat-capacity measurements were performed using a graphite foam substrate of 47 ± 1 m^2 area as determined from a N_2 adsorption isotherm at liquid-N_2 temperature.[11] The calorimeter cell was designed to acquire data in a relatively short time, sacrificing high accuracy at each point. The design and operation of this system has been described.[4,12] Heat capacities and coverages (Nk_B) are reported in units of mJ/K, where N is the total number of molecules at a particular coverage and k_B is Boltzmann's constant. For conversation to more conventional units, 4.1 ± 0.1 mJ/K in this cell corresponds to $\rho = 1$, the $(\sqrt{3} \times \sqrt{3})R30°$ commensurate density for first layer hydrogens, Kr, N_2, and heliums on graphite.

The adsorption isotherms were performed in a computer-controlled isotherm station using the uncompressed exfoliated graphite as the substrate. This substrate is highly homogeneous (not crushed by compression) and above all, has a much smaller impedance to gas flow than any of the exfoliated graphites available in sheet form. The trade off is that it has a very small area-volume ratio unless one compresses the crystallites into containers, which it some extent degrades their homogeneity and increases their flow impedance. We slightly compressed them into a copper cell welded to a stainless steel fill line which could be baked to 400 °C. Two series of measurements were performed. In the first series, the initial test of the isotherm cryostat, one second layer and the third and fourth layer sets of isotherms were measured. After improvements in the operation of the cryostat, the adsorption cell was rebaked, a new N_2 isotherm was measured, and the second layer of HD isotherms were measured in great detail exploiting the resolution of the station. An identical difference in the cell area was detected by both N_2 and HD isotherms between the two sets. For calculating isosteric heats, Sec. IV, the coverages of the first set of isotherms have been adjusted by the ratio of the areas to the same area as the second set. The isotherms coverage is reported in cm^3 STP. A coverage of 9.63 cm^3 STP in the isotherm cell corresponds to 12.2 mJ/K in the heat-capacity cell.

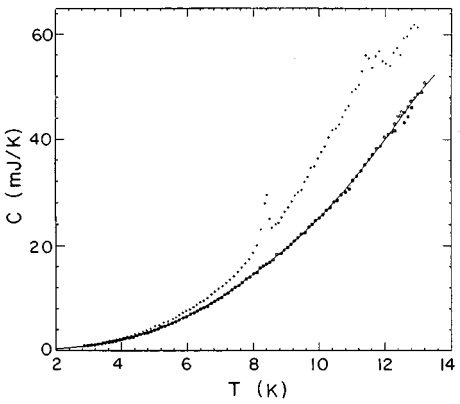

FIG. 1. Background heat capacity of the empty cell and its seventh-order polynomial fit, and total heat capacity of the cell plus an HD film with coverage $Nk_B = 10.06$ mJ/K.

The computerized adsorption system uses two Baratron capacitance manometers, one for the cell side volume and one for the dosing volume, with a computer-controlled valve (V_3) in between them. This makes the cell side volume outside the cryostat to be essentially the volume of the Baratron head rather than the usually large and tortuous shot volume when a single manometer is used, and helps achieve pressure equilibration in relatively short times.

The QENS experiments were performed on the time-of-flight spectrometer MIBEMOL at the Laboratoire Léon Brillouin in Saclay (France), using three short-time allocations over a 1-yr period. The incident wavelength was 8 Å (1.28 meV) with a triangular-shaped resolution of 40 μeV. The scattered beam was measured by 12 detector banks located at various scattering vectors Q ranging from 0.4 to 1.4 $Å^{-1}$. The film's scattering spectra were obtained by subtracting the background due to the cell plus the bare graphite substrate from the spectra taken with different dosings. The area of each one of the three cells used was determined by either a CH_4, a N_2, or an HD isotherm, and for one of the cells by N_2 and HD isotherms. The Papyex used to obtain the data reported in Sec. III has a coherence length of approximately 300 Å. QENS measurements from mobile, partial monolayer HD films are time consuming due to resolution, lack of scatterers, and neutron flux limitations, thus only one coverage corresponding to $\rho \approx 2.63$ (about 1.7 layers) was measured.

III. RESULTS

(a) Heat capacity of HD/HD/Gr. The background heat capacity of the empty calorimeter was measured in the temperature range $2.8 < T < 13.2$ K, and fitted by a seventh-order polynomial.

HD gas was introduced into the sample cell at 20 K, and the HD film was then annealed at 16 K for ≈ 5 h before the cell was gradually cooled down to ≈ 3.4 K. We measured a total of 14 heat-capacity scans for coverages from about 0.95 monolayer up to about 2 monolayers, and for $3.5 < T < 13$ K. One of such scans for a film with $Nk_B = 10.06$ mJ/K is shown in Fig. 1 along with the background heat capacity and its seventh-order fit.

The background-substracted film heat capacities of a few

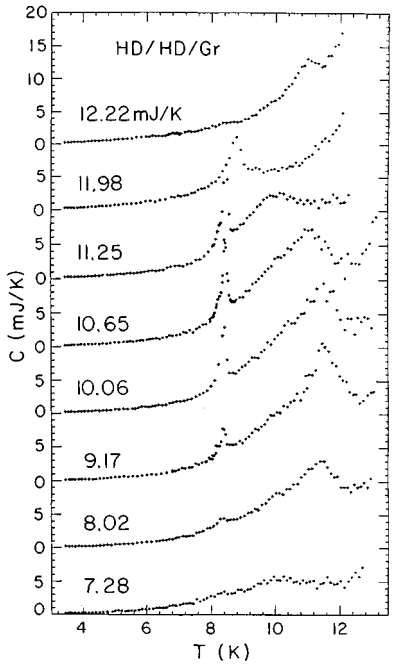

FIG. 2. Heat-capacity scans for a few HD coverages, with the empty cell background subtracted. Note the heat-capacity vertical shift between heat-capacity scans, introduced for graph clarity.

selected HD coverages are shown in Fig. 2. The heat capacity from desorption at the high-T end has not been substracted.

From the heat-capacity data, we propose the coverage-temperature phase diagram for the second-layer HD on graphite shown in Fig. 3. The sharp peaks in Fig. 2 at an almost constant temperature $[T_t(2D)=8.44\ \mathrm{K}]$ occur at the S-L-V second-layer triple point (see the QENS section below). The broader peaks in Fig. 2 at temperatures higher than the triple line map out the boundary of the L-V coexistence region, which ends at the critical point $T_c(2D)\approx 11.45$ K.

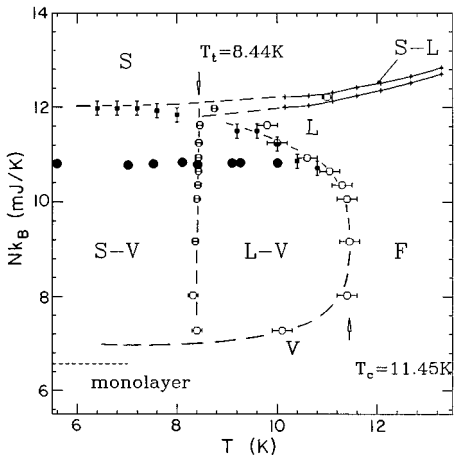

FIG. 3. Proposed phase diagram for (second layer) HD/HD/gr. Phase boundaries determined by ○, heat capacity features (horizontal error bars); ■, heat-capacity isotherms (vertical error bars); +, adsorption isotherms. Nk_B is the total HD coverage. ●, location of QENS measurements.

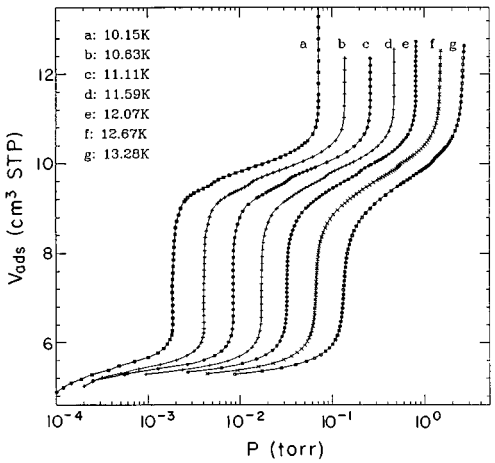

FIG. 4. Second-, and beginning of third-, layer volumetric vapor-pressure isotherms of HD on graphite from the second run. The temperatures are shown for each isotherm. Lines are guides to the eye.

The total heat capacity at constant T within a two-phase coexistence region should be linear with coverage.[13] The ending points of the linear regions in the heat-capacity isotherms trace out the two-phase boundaries, shown in Fig. 3 by square symbols. The boundary determinations by the heat-capacity peaks and heat-capacity isotherms complement each other and show reasonable agreement. Due to the limited number of coverages measured at the beginning of the second layer, the lower boundaries of the S-V and L-V regions cannot be determined very accurately.

The 11.98 and 12.22 mJ/K runs identify the second-layer melting line at coverages above triple-point coexistence. The S-L coexistence region was mapped more carefully by the adsorption isotherms described below.

(b) Adsorption isotherms. Vapor-pressure isotherms complement heat-capacity measurements. When desorption into the dead volume of the calorimeter is insignificant, a heat-capacity measurement traces a constant coverage path, i.e., a line parallel to the T axis in a coverage-temperature phase diagram like Fig. 3. Heat-capacity features clearly identify triple lines and L-V coexistence. Adsorption isotherms follow, in Fig. 3, a path perpendicular to the heat capacity. They are useful in identifying layer-by-layer growth and two-phase coexistence regions, to characterize surface quality and to measure adsorption energies.[14]

Seven second-layer isotherms were measured between 10.15 to 13.28 K, see Fig. 4. Pressures have been corrected for the thermomolecular effect. The main vertical step corresponds (for the three lowest temperatures) to the L-V coexistence region (see QENS section below). Between the second and third layers we found very small ''almost vertical'' steps corresponding to S-L coexistence. Figure 5 shows a blowup of Fig. 4 around these steps. They move to higher coverage and further away from the main isotherm step as the temperature increases. The dashed lines map out the S-L coexistence region in the temperature range measured. In earlier vapor-pressure isotherm studies on bilayer H_2 and HD on MgO,[5,6,15] the S-L coexistence regions were clearly identified by sizable steps in the isotherms, rather different than for the HD/HD/gr system.

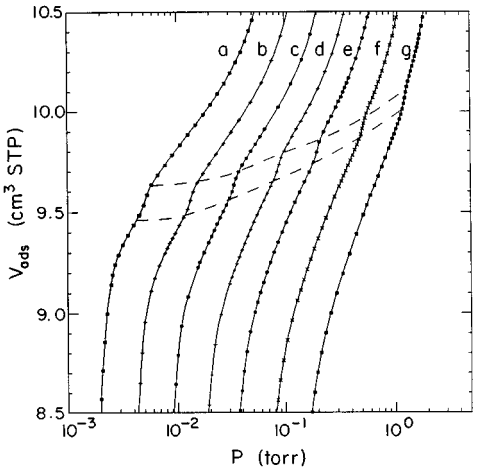

FIG. 5. Isotherm substeps and the *S*-*L* coexistence region (between dashed lines) in the second layer HD on graphite. *a*, 10.15 K; *b*, 10.63 K; *c*, 11.11 K; *d*, 11.59 K; *e*, 12.07 K; *f*, 12.57 K; *g*, 13.28 K.

We have incorporated this determination of the melting line into Fig. 3 by scaling coverages using the scaling of Sec. II (the melting peak at $Nk_B=12.22$ mJ/K and 11.0 K from the heat-capacity measurements and the middle point of the substep in the 11.11 K isotherm at $V_{\rm ads}=9.63$ cc-STP, neglecting the small temperature difference). The *S*-*L* coexistence region from the isotherms is shown by the solid lines. It should be pointed out that there is a 3% discrepancy between this scaling and one using N_2 isotherms at 77.6 K which perhaps could be caused by different substrate heterogeneities. Details are reported in Liu's dissertation.[16]

From the adsorption isotherms shown, and the third and fourth layer ones (not shown but available from PSE or OEV) it is also possible to obtain the critical points of the second, third, and fourth layers by calculating their slopes above T_c as a function of T at fixed surface (critical) density. The inverse slope (inverse compressibility) should go to zero at T_c. Estimates of T_c obtained this way have larger uncertainties than when obtained with heat capacity because inverse slopes decrease with an (Ising) power law, and substrate heterogeneities make the final inverse slope finite.[17] This method gives critical temperatures of 11.8 (higher than the 11.45 K obtained from heat capacity), 12.3, and 12.0 K (± 0.2 K), respectively, for the second, third, and fourth layers. The third- and fourth-layer T_c's are in fairly good agreement with values determined by Wu and Hess using ellipsometric adsorption isotherms on graphite (12.2 and 12.5 K, respectively).[18] One may also obtain T_t(2D) of the second layer by extrapolating to low P and T the loci of the two-phase coexistence pairs $(P,1/T)$ from the vertical steps of the isotherms. We obtain $T_t(2D)\approx 8.42\pm 0.10$ K, in excellent agreement with the heat-capacity results.

(c) QENS. The HD dose studied corresponds to about 1.7 layers, close to the top of the *L*-*V* coexistence region (see Fig. 3, solid symbols). Data were taken at selected temperatures between 2 and 10 K.

A spectrum (minus background) is shown in Fig. 6 for $Q=0.627$ Å^{-1} at 9.25 K, above T_t(2D). The central triangular peak is due to the resolution-limited solid HD scattering. The wings at the foot of the triangular peak come from

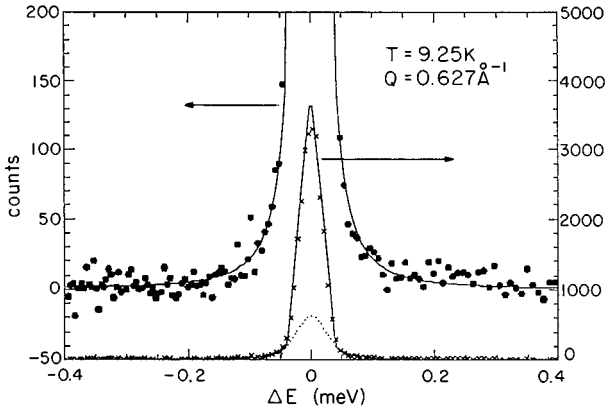

FIG. 6. QENS spectrum (minus background) for a bilayer HD film at 1.7 layers coverage, $Q=0.627$ Å^{-1} at $T=9.25$ K, and best fit using the model described in text.

the mobile fraction of HD, x. Spectra at 9, 9.25, and 10 K, i.e., above T_t(2D), all show the broad component. At 8.1 K, i.e., somewhat below T_t(2D), very small wings are observed. One complete MIBEMOL time allocation (6 days) was dedicated to taking a background and spectrum at 2 K, see below.

The QENS spectra (minus background) are analyzed as a sum of a δ function originating in the solid HD monolayer (s) and a Lorentzian function which comes from the incoherent scattering of a mobile phase, this sum convoluted with the triangular instrument resolution. We assume that at the temperature of the measurements the HD molecule is effectively a free rotator. The scattering law, $S(Q,\omega)$, consists of two terms. The first one is proportional to the solid fraction $(1-x)$ of the film, and the second one to the mobile fraction, x, such that

$$S(Q,\omega)=j_0^2(Qr)e^{-Q^2\langle u^2\rangle}[(1-x)\delta(\omega)+xL(Q,\omega)], \qquad (1)$$

where $\hbar\omega=E-E_0$ is the gain or loss of energy of the neutron with respect to the incident energy E_0. The j_0 spherical Bessel function describes the isotropic rotational motion of the HD molecule with a gyration radius $r=0.37$ Å. The exponential term is the Debye-Waller factor. It is set here to unity because the data reduction was done only at small Q (less than 1 Å^{-1}), i.e., in the Q range where the neutron statistics is fairly good. The Lorentzian function $L(Q,\omega)$ is given by

$$L(Q,\omega)=\pi^{-1}f(Q)/(f^2(Q)+\omega^2) \qquad (2)$$

with $f(Q)$ depending on the model, i.e.,

$$f(Q)=D_TQ^2\sin^2\tau \qquad (3)$$

for a two-dimensional Brownian liquid. D_T is the translation diffusion coefficient of the fluid, τ is the angle between the normal to the (0001) individual graphite surface and the scattering vector Q. Equation (1) has to be averaged over the orientation distribution of the graphite crystallites and convoluted with the instrumental resolution before fitting to the recorded spectra. It has only two adjustable parameters, x, the film mobile fraction, and D_T, the translational diffusion coefficient of the mobile phase. A more complete description of the procedure used has been written by Coulomb *et al.*[19]

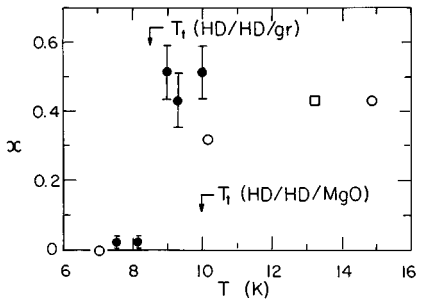

FIG. 7. The mobile fraction of a monolayer, x, as determined from QENS measurements. ●, HD/HD/gr, this experiment; ○, HD/HD/MgO, 1.6 layers; and □, HD/HD/MgO, 1.9 layers, from Ref. 8.

The most important outcome of the QENS measurements is that they confirm the existence of the second-layer 2D liquid on top of a first layer solid. Using Eq. (1) we have calculated x and D_T from best fits to the QENS spectra. Results are shown in Figs. 7 and 8. The mobile fraction is approximately constant in the L-V coexistence region and corresponds to about half a monolayer, as expected. At 8.1 K and below there are very small wings on the QENS spectra, which, when analyzed with the same model of Eq. (1), give $x \approx 0.02 \pm 0.01$ below the triple-point temperature.

The measured translational diffusion coefficients in Fig. 8 at 9–10 K are smaller but of comparable magnitude to those for 3D liquid HD at slightly above its triple point ($\approx 5\times10^{-5}$ cm^2 s^{-1}, see Zeppenfeld *et al.*[7]). They are also comparable to those measured for multilayer HD on MgO at about the same temperature. In Fig. 8 we show with an open circle and the dash-dotted line the results of Maruyama *et al.*[8] for 1.6 layers of HD/MgO. The dash-dotted line corresponds to a fitting of the form $D_T \approx D_0 \exp(-16\ \mathrm{K}/T)$ through the MgO data. A similar exponential fit through the three HD/HD/gr points (dashed line) gives an activation energy of 55 K. We do not have precise enough data to decide if the activation energy is actually this high. An extension of the HD/MgO line to lower T would also go through the error estimates of the three HD/HD/gr points.

We do not have a simple explanation for the very small wings at the foot of the resolution limited QENS central peak

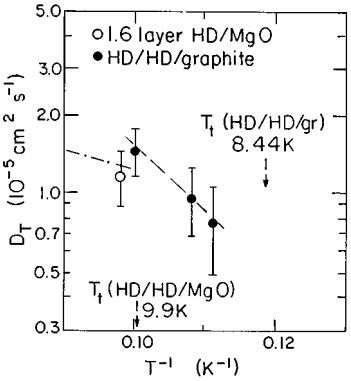

FIG. 8. Translational diffusion coefficient for the liquid HD monolayer, determined from the QENS measurements, see text. ●, HD/HD/gr, this experiment. ○, HD/HD/MgO, 1.6 layers, from Ref. 8.

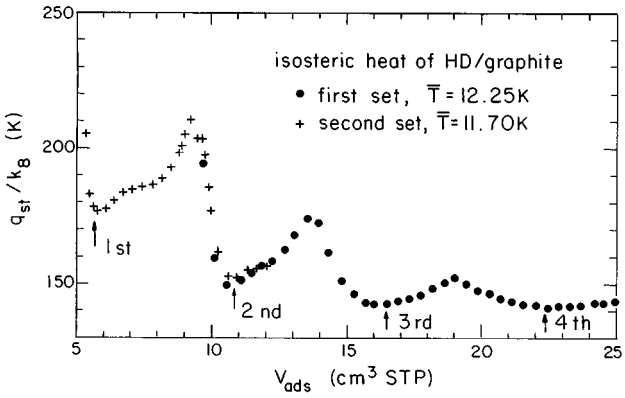

FIG. 9. Isosteric heat of adsorption vs HD coverage at $\bar{T} = 12.25$ K from first set of isotherms, and $\bar{T} = 11.70$ K from the second set of isotherms.

below the triple point, which persist down to 2 K. If the decrease of D_T with temperature shown in Fig. 8 is exponential, the wings in the QENS spectra at 2 K from a liquid fraction would be much narrower in energy than the resolution of the spectrometer for activation energies between 16 and 55 K. A small amount of 2D vapor (in equilibrium with the 2D solid) could have the right mobility at 2 K to give transit times in the range of 10^{-11} s. We have measured a few H_2 (not HD) heat-capacity runs around 2 K at H_2 monolayer completion and beginning of the second layer, which show that the S-V second-layer coexistence does not start until a few hundredths of the second layer are deposited, but the data are sparse and not conclusive.

IV. FURTHER ANALYSIS AND DISCUSSION

The proposed phase diagram, Fig. 3, is similar in form to those of 3D van der Waals systems, and to those of H_2/H_2/gr, D_2/D_2/gr,[2] and H_2/H_2/MgO.[5] The triple-point $T_t = 8.44$ K is in between 5.96 K for H_2/H_2/gr and 11.0 K for D_2/D_2/gr, and is about 1.5 K lower than the 9.9 K for HD/HD/MgO.[6] This is consistent with the graphite vs MgO substrate trend mentioned in the Introduction.

A thermal property which may be calculated directly from the isotherms is the isosteric heat of adsorption, defined as[13]

$$q_{\mathrm{st}} \equiv k_B T^2 (\partial \ln P / \partial T)_{N_f, A}, \tag{4}$$

where N_f and A denote the film coverage and adsorption area of the substrate. At very low coverages where the lateral interaction between adatoms can be neglected, the isosteric heat is simply related to the binding energy (ε_0) and kinetic energy by

$$q_{\mathrm{st}} = \varepsilon_0 + \alpha(k_B T) \tag{5}$$

with $\alpha = 3/2$ for a 2D ideal gas on a flat surface and $\alpha = 1/2$ for a gas molecule harmonically bound to an adsorption site. In the L-V coexistence region, q_{st} includes the latent heat of 2D evaporation which is independent of the coverage.

Figure 9 shows q_{st} vs V_{ads} for the two sets of isotherms, obtained by using Eq. (4). We averaged over all the isotherms of Fig. 4 (10.15–13.28 K), and over a comparable

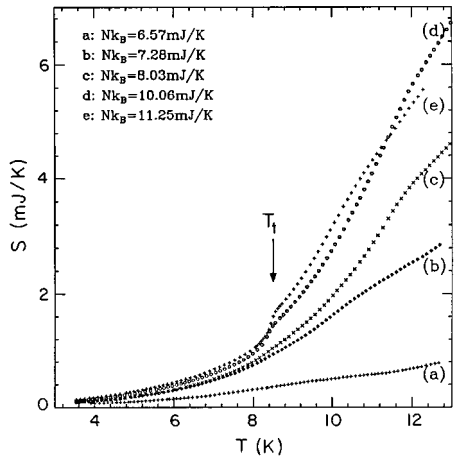

FIG. 10. Calculated entropies of a few selected HD coverages. The coverages shown are the total HD coverages. The inflection points are due to triple-point melting (8.44 K) or evaporation at the L-V boundary.

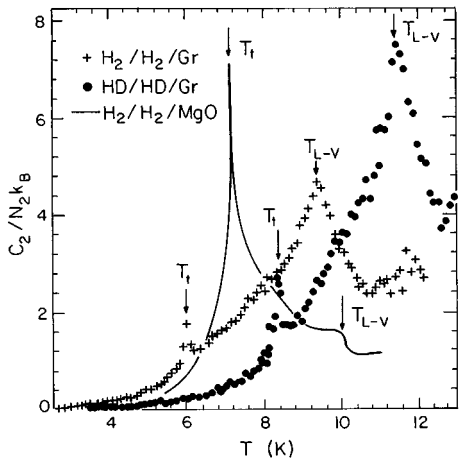

FIG. 11. Second-layer specific heats of three hydrogen bilayers on graphite or MgO, each with about 0.4 monolayer in the second layer, see text.

range of temperatures from the third, fourth, and partial fifth layers to reduce the scatter. The average temperatures are $\overline{T}=11.70$ K for the first set, and $\overline{T}=12.25$ K for the second set. There are dips in $q_{\rm st}$ at layer completions, which give $q_{\rm st}\approx 177$, 152, 143, and 141.5 K (± 2 K) at the beginning of the second, third, fourth, and fifth layers, indicating the decrease of the total effective potential and growth towards the 3D heat of sublimation of HD.[20] The first plateau in $q_{\rm st}$ in the second layer is due to the three lowest temperature isotherms used in the calculation being in the L-V region, and the rise which follows is due to freezing and L-S coexistence. The third layer seems to go through a similar pattern. The fourth and fifth layers are not well resolved, but they also show rises towards monolayer completion.

In Ref. 4, Liu *et al.* discussed the procedures to calculate the entropy (S), solid fraction in the S-V coexistence region (N_{2s}), and heat of fusion (q) from heat-capacity measurements. We use here the same procedure. Entropies are calculated numerically by extrapolating the heat-capacity data to $T=0$ K using a quadratic fit to the lowest measured points, then integrating C/T from $T=0$ K to the desired temperature. Calculated entropies of a few selected coverages are shown in Fig. 10. Curve (a) is for the coverage $Nk_B=6.57$ mJ/K, approximately a complete HD monolayer. The rapid rise at T_t(2D) of the bilayer, and the slight inflexion at the end of the bilayer L-V coexistence are clearly visible.

To estimate the heat of fusion, q, at the triple point we draw a smooth line under the triple-point heat-capacity peaks and integrate numerically the area under those peaks. The number of HD molecules in the second layer which melt at the triple point is given by the lever rule

$$N_{2s}=[(N_s^0-N_1)/(N_s^0-N_v^0)](N-N_v^0), \qquad (6)$$

where $N_s^0k_B=12.0$ mJ/K and $N_v^0k_B\approx 7.0$ mJ/K are the upper and lower boundaries of the S-V region, Nk_B the total coverage, and $N_1k_B=6.57$ mJ/K the coverage of the complete first layer. As mentioned earlier, the lower boundary $N_v^0k_B$ is not as well defined. We obtain $q=5.2$ J/mol, and a molar entropy change $\Delta s=0.61$ J/mol K. Using a similar procedure it has been calculated[2] that Δs at the triple point for H_2/H_2/gr is 0.65 J/K mol, and for D_2/D_2/gr is 0.61 J/K mol, about the same as for HD/HD/gr.[2] We note also that the entropy change in H_2/H_2/MgO, measured by Ma *et al.*, is 2.0 J/mol K, three times larger than for the three systems so far studied on graphite,[6] and the entropy change for 3D HD at its triple point is 9.58 J/K mol, much larger than for the 2D systems.

The comparison between bilayer films on graphite and MgO is particularly interesting. Not only is T_t(2D) about 1.5 K lower on graphite than on MgO, but both Δs and q on graphite are considerably less than those on MgO. This can be seen from the strikingly different specific heats on the two substrates. Three second-layer specific heats (with the first-layer heat capacity subtracted) for films of about equal coverages (0.4 of a second monolayer), all measured in our cryostat, are plotted in Fig. 11. The two specific heats on graphite are similar in form, with small triple-point peaks (small entropy changes) and large transition peaks at the L-V phase boundaries, but the one on MgO has a very large triple-point peak and very small L-V signal. This indicates that there is not a great deal of difference between the liquid and the solid bilayer on the graphite, and this is confirmed by the narrow solid-liquid coexistence region in the isotherms of HD/HD/gr, see Fig. 5, where there is a change in density of about 1.6% of a monolayer between the liquid and the solid. By contrast, there is a 4% of a monolayer density change between the 2D liquid and the 2D solid for a comparable adsorption isotherm of HD/HD/MgO. From the increased ordering of the liquid on graphite, we expected that the mobility in the liquid phase of the second layer of HD/HD/gr would be considerably smaller than on HD/HD/MgO,[8] but this did not turn out to be the case, see Fig. 8. Both fluids appear to be equally mobile around 10 K within the sensitivity of the QENS measurements.

In the phase diagram of Fig. 3 we interpret the high coverage region, $Nk_B>12$ mJ/K, as a single solid phase. We explore the solid with the 2D Debye model. The low-temperature specific heat varies as[13]

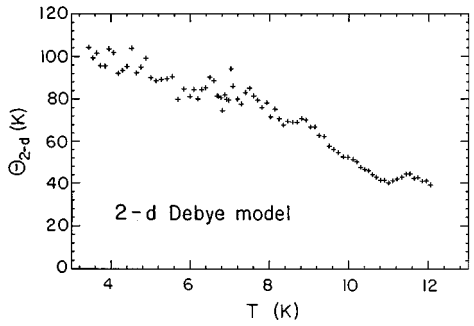

FIG. 12. Calculated effective 2D Debye temperatures, Θ_{2D}, for the second-layer specific heat of the HD film with $Nk_B = 12.22$ mJ/K.

$$C/N_2k_B \sim 28.85(T/\Theta_{2D})^2, \tag{7}$$

where Θ_{2D} is the Debye temperature, C and N_2k_B are the heat capacity and coverage of the second layer.

Using the 12.22 mJ/K run, entirely within the solid phase, the second-layer heat capacity can be roughly obtained by subtracting the heat capacity of the first layer ($N_1k_b = 6.57$ mJ/K). We force Eq. (7) through each point of the second-layer specific heat. Results are displayed in Fig. 12. The Debye temperature is not constant, decreasing with increasing temperature. The $T = 4$ K value of $\approx 100 \pm 4$ K is somewhat smaller than the 3D value of 110 K at the same temperature, but the temperature dependence of Θ_{2D} is similar to, albeit more pronounced than, the one in 3D for H_2, see Fig. 51 of Silvera's review.[21] The likely formation of an HD common oblique structure as proposed by Wiechert[2] for bilayer H_2 and D_2, the second layer not being a 2D solid ''freely floating'' on the solid first layer, will have to be considered in theoretical treatments of the solid.

Finally, Fig. 13 shows a summary of our current knowledge of 2D S-L-V triple, and L-V critical point temperatures. The figure has been drawn as a dimensionless $T_c(2D)/\epsilon$ or $T_t(2D)/\epsilon$ vs the quantum parameter $\eta = \hbar^2/m\sigma^2\epsilon$, a corresponding states picture at the quantum limit. In this equation, m is the HD mass, and $\sigma = 2.92$ Å and $\epsilon = 37$ K are the Lennard-Jones values for the parameters reported by Nosanow.[22] We believe that the large fractional difference between the values of the phase-transition temperatures for the same isotopic molecule on the different substrates is a consequence of variations in the effective interaction between the molecules induced by each substrate, and possibly, differences in effective mass caused by the substrate corrugation. We note that in this very quantum regime solidification of the hydrogen molecules under their own 2D vapor pressure occurs near the end of the allowed $T_t^*(2D)$ vs η value for Bosons are calculated by Ni and Bruch.[23]

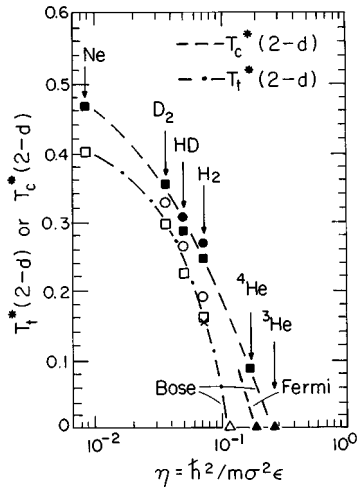

FIG. 13. Quantum corresponding states picture showing the 2D reduced temperature triple and critical points currently known for H_2, HD, and D_2 molecules (from Refs. 2,5,6, see Introduction, and this work). $T_c(2D)$ for ^{4}He adsorbed on H_2/H_2/gr from Ref. 24. Limits at $T = 0$ K for solidification from Ni and Bruch (Ref. 23) and for L-V critical points from Miller and Nosanow (Ref. 25). Solid symbols correspond to critical points, open symbols to triple points, squares to films on graphite and circles to films on MgO. ×, H_2/D_2/gr from Ref. 4. Neon points from Huff and Dash (Ref. 26). Lines are guides to the eye.

ACKNOWLEDGMENTS

We acknowledge support for this research from the NSF, Grant Nos. DMR 92 20729 and INT 90 15952, and CNRS. Three of us (Y.M.L., J.G.D., O.E.V.) would like to thank the hospitality of the CRMC2 during the measurement and analysis of the QENS data and the writing of this article.

*Present address: MTL-10, MSK764, Los Alamos National Laboratory, Los Alamos, NM 87545.

† Present address: Department of Physics, University of Massachusetts, Amherst, MA 01003.

[1] H. Wiechert, Physica B **169**, 144 (1991).

[2] H. Wiechert, in *Excitations in Two-Dimensional and Three-Dimensional Quantum Fluids*, edited by A. G. F. Wyatt and H. J. Lauter (Plenum, New York, 1991), p. 499.

[3] F. C. Liu, Y. M. Liu, and O. E. Vilches, J. Low Temp. Phys. **89**, 649 (1992).

[4] F. C. Liu, Y. M. Liu, and O. E. Vilches, Phys. Rev. B **51**, 2848 (1995).

[5] J. Ma, D. L. Kingsbury, F. C. Liu, and O. E. Vilches, Phys. Rev. Lett. **61**, 2348 (1988).

[6] O. E. Vilches, F. C. Liu, D. L. Kingsbury, J. Ma, M. Bienfait, J. Suzanne, J. M. Gay, M. Maruyama, P. Zeppenfeld, D. Degenhardt, H. J. Lauter, F. Rieutord, and G. Coddens, in *Excitations in Two-Dimensional and Three-Dimensional Quantum Fields* (Ref. 2), p. 477.

[7] P. Zeppenfeld, M. Bienfait, F. C. Liu, O. E. Vilches, and G. Coddens, J. Phys. (France) **51**, 1929 (1990).

[8] M. Maruyama, M. Bienfait, F. C. Liu, O. E. Vilches, and F. Rieutord, Surf. Sci. **283**, 333 (1993).

[9] E. K. Jeong, Ph.D. dissertation, Washington University, 1991; and E. K. Jeong, B. Ouyang, R. E. Norberg, P. A. Fedders, and M. S. Conradi, Phys. Rev. Lett. **69**, 2348 (1992).

[10] J. Nyéki, R. Ray, V. Maklusov, M. Siqueira, B. Cowan, and J. Saunders, J. Low Temp. Phys. **101**, 279 (1995); M. Siqueira, C.

P. Lusher, B. P. Cowan, J. Cowan, and J. Saunders, Phys. Rev. Lett. **71**, 1407 (1993).
[11] M. H. W. Chan, A. D. Migone, K. D. Miner, and Z. R. Li, Phys. Rev. B **30**, 2681 (1984).
[12] F. C. Liu, Ph.D. dissertation, University of Washington, Seattle, 1992.
[13] J. G. Dash, *Films on Solid Surfaces* (Academic, New York, 1975).
[14] R. E. Ecke and J. G. Dash, Phys. Rev. B **28**, 3738 (1983).
[15] J. Ma., Ph.D. dissertation, University of Washington, Seattle, 1989.
[16] Y. M. Liu, Ph.D. dissertation, University of Washington, Seattle, 1993. Data tables and other information in this dissertation are available from the authors, and from University Microfilms, 1490 Eisenhower Place, P.O. Box 975, Ann Arbor, MI 48106.
[17] R. E. Ecke, J. Ma, A. D. Migone, and T. S. Sullivan, Phys. Rev. B **33**, 1746 (1986).
[18] H. Wu and G. B. Hess, Bull. Am. Phys. Soc. **39**, 795 (1994).
[19] J. P. Coulomb, M. Bienfait, and P. Thorel, J. Phys. (Paris) **42**, 293 (1981).
[20] P. C. Souers, *Hydrogen Properties for Fusion Energy* (University of California Press, Berkeley, 1986), p. 112. The heat of sublimation is calculated to be 146 K at 12 K, and 141.7 K at 10 K, after vapor-pressure data of H. J. Hoge and R. D. Arnold, J. Res. Natl. Bur. Stand. **47**, 63 (1951). Our q_{st} at about 12 K is 3% lower than the quoted value. Part of the discrepancy may be due to difficulties in obtaining an accurate thermomolecular pressure correction.
[21] I. F. Silvera, Rev. Mod. Phys. **52**, 393 (1980).
[22] L. H. Nosanow, J. Phys. (Paris) Colloq. **41**, C4-1 (1980).
[23] X. Z. Ni and L. W. Bruch, Phys. Rev. B **33**, 4584 (1986).
[24] P. S. Ebey and O. E. Vilches, J. Low Temp. Phys. **101**, 469 (1995).
[25] M. Miller and L. H. Nosanow, J. Low Temp. Phys. **32**, 145 (1978).
[26] G. B. Huff and J. G. Dash, in *Proceedings of the International Conference on Low Temperature Physics (LT 13)*, edited by R. H. Kropschot and K. D. Timmerhaus (Plenum, New York, 1974), p. 165.